Threshold Excitation of Short-Lived Atomic Inner-Shell Hole States with Synchrotron Radiation

G. Bradley Armen, Teijo Åberg,[a] Jon C. Levin, and Bernd Crasemann
Department of Physics and Chemical Physics Institute, University of Oregon, Eugene, Oregon 97403

and

Mau Hsiung Chen
Lawrence Livermore National Laboratory, Livermore, California 94550

and

Gene E. Ice
Metals and Ceramics Division, Oak Ridge National Laboratory, Oak Ridge, Tennessee 37830

and

George S. Brown
Stanford Synchrotron Radiation Laboratory, Stanford, California 94305
(Received 9 January 1985)

The Xe L_3-M_4M_5 ($^1G_4$) Auger spectrum, photoexcited in the vicinity of the L_3 edge, has been measured as a function of photon energy. The *nd* spectator-electron satellite lines show resonant behavior. The diagram line exhibits the largest ($\gtrsim 1$ eV) post-collision interaction shift yet observed. For comparison with the data, the first fully quantum-mechanical calculation of the post-collision interaction in deep inner-shell Auger decay is performed, based on a resonant-scattering approach that involves a complete summation over intermediate L_3 one-hole states.

PACS numbers: 32.80.Hd, 32.80.Fb

In threshold excitation of short-lived, deep atomic inner-shell hole states, ionization and decay cannot be treated as distinct processes. Directly at threshold, photoionization and radiationless deexcitation occur in a single process, the resonant Raman effect.[1] Above threshold, excitation and deexcitation are still linked by post-collision interaction (PCI), in which the Auger decay takes place under the influence of the Coulomb field of the receding photoelectron and some of the photoelectron's energy is transferred to the Auger electron. Measurements of the Auger spectrum excited near threshold can therefore probe the dynamics of inner-shell transitions and provide a stringent test of the semiclassical PCI theory[2] which has been shown to be valid in the limit of long hole-state lifetimes.[3] The first fully quantum-mechanical calculation of PCI becomes possible, based on resonant scattering theory,[4,5] since the intermediate-state summations can be restricted to states associated with the initial inner-shell hole.

Here we report on an investigation in which highly monochromatized, hard synchrotron radiation was tuned through the L_3 threshold of Xe and the L_3-M_4M_5 ($^1G_4$) Auger decay including the *nd* ($n \geqslant 5$) spectator-electron satellite distribution was observed. The peak positions and widths of the $n=5$ and $n=6$ spectator lines were measured as functions of photon energy. The evolution of the M_4M_5 double photoionization peak into the Auger diagram line was found to be strongly blended with the $n \geqslant 6$ spectator satellites in the excitation-energy range from $E_{\text{exc}} = -0.5$ eV to $+5$ eV with reference to the ionization threshold, producing a large apparent PCI shift (~ 3 eV). We compare this result with predictions from the resonant scattering theory at $E_{\text{exc}} = +3$ eV. Above $E_{\text{exc}} \cong +5$ eV, the PCI shift is solely due to distortion of the diagram-line shape, so that comparison with both the resonant scattering and semiclassical theories becomes possible.

In the experiment, performed in the Stanford Synchrotron Radiation Laboratory, x rays from an eight-pole wiggler operating at 14 kG were focused onto a Xe jet by a Pt-coated doubly curved toroidal mirror. A narrow energy band (~ 0.6 eV) was selected with a tunable Si (111) $(1,-1)$ double-crystal monochromator. The energy spectrum of electrons emitted from the Xe target was measured with a double-pass cylindrical-mirror analyzer.[1] We take the asymptotic Auger diagram-line energy $\epsilon_A^0 = 3365.9 \pm 0.2$ eV as reference for the PCI shift. Typical Auger spectra excited at $E_{\text{exc}} = -2$ eV and $+1.5$ eV are shown in Fig. 1.

In the resonant scattering theory[4,5] of the PCI effect, a consistent treatment of threshold phenomena is achieved by interpreting the Auger transition $[n_il_i] \rightarrow [n_fl_f, n_{f'}l_{f'}]$ as a resonance in the double-electron photoionization of the n_fl_f and $n_{f'}l_{f'}$ subshells.[6] As the incident-photon energy approaches the ionization energy I_i of the n_il_i threshold, spectator transitions of the type $[n_il_i]nl \rightarrow [n_fl_f, n_{f'}l_{f'}]nl$ start to appear because of $n_il_i \rightarrow nl$ excitations. At the threshold, the spectator lines blend into the rapidly increasing double-ionization peak, for which the cross section at large excitation energies $E_{\rm exc} = \omega - I_i$ becomes the product of the $n_il_i \rightarrow \epsilon l$ single-electron photoionization cross section and the Auger decay probability $\Gamma(\epsilon_{\rm A}^0)$ for the $[n_il_i] \rightarrow [n_fl_f, n_{f'}l_{f'}]^{2S+1}L_J$ transitions with energy $\epsilon_{\rm A}^0$. Close to threshold, the Auger decay cannot be treated as an independent process because the emission of the Auger electron is affected by transitions from the single- to double-hole $n(\epsilon)l$ states. The double photoionization cross section is

$$\frac{d^2\sigma}{d\epsilon\, d\epsilon_{\rm A}} = \frac{4\pi\alpha\omega_0}{3}\Gamma(\epsilon_{\rm A}^0)\int_0^\infty |\langle\epsilon|\tau'\rangle|^2 N(\omega-\omega_0)\delta(\omega-\epsilon-\epsilon_{\rm A}-I_{ff'})\,d\omega, \qquad (1)$$

where $N(\omega-\omega_0)$ is the distribution function of the incident photons (normalized to unity), $\epsilon_{\rm A}$ is the Auger-electron energy, and $I_{ff'}$ is the ionization energy of the final double-hole state. We have placed the slowly varying factor $\omega_0\Gamma(\epsilon_{\rm A})$ outside the integral. If the continuum wave function $|\epsilon\rangle$ is replaced by the discrete-state wave function $|n\rangle$ in the overlap matrix element $\langle\epsilon|\tau'\rangle$, the double-ionization cross section reduces to the cross section $d\sigma_n/d\epsilon_{\rm A}$ for emitting an Auger electron and placing a spectator electron in the excited state nl. In Eq. (1), we have

$$|\tau'\rangle = \sum_{n'=n_{\rm min}}^{\infty} \frac{|n'\rangle\langle n'||r||0\rangle}{E_{\rm exc}+\tau_{n'}+i\Gamma_i/2} + \int_0^\infty \frac{|\tau\rangle\langle\tau||r||0\rangle\,d\tau}{E_{\rm exc}-\tau+i\Gamma_i/2}, \qquad (2)$$

where each $|\tau(n')\rangle$ must be evaluated in the field of the singly ionized atom with an n_il_i hole, in contrast to the final $|\epsilon(n)\rangle$ double-hole states. In Eq. (2), Γ_i is the total decay width of the $[n_il_i]$ hole state, and $\langle\tau(n')||r||0\rangle$ is the reduced radial dipole matrix element.

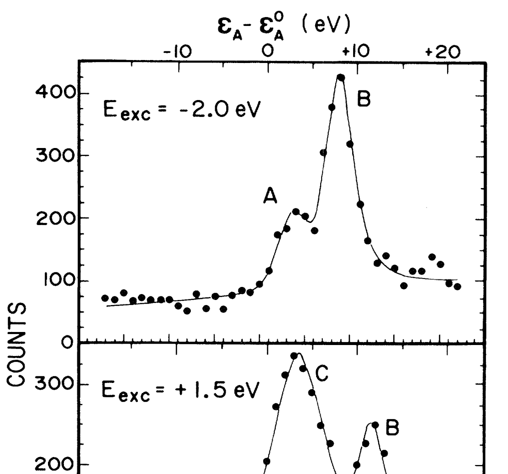

FIG. 1. Xenon L_3-M_4M_5 ($^1G_4$) Auger-electron spectrum, excited with synchrotron-radiation photons of energy 2.0 eV below the Xe L_3 binding energy (top) and 1.5 eV above the Xe L_3 binding energy (bottom). Feature A consists primarily of nd ($n \geq 6$) satellites, with a slight admixture of the PCI-shifted diagram line; feature B is the $5d$ spectator satellite, and feature C consists of the PCI-shifted diagram line, with an admixture of nd ($n \geq 6$) satellites.

Close to threshold, the Auger-electron emission intensity as a function of $\epsilon_{\rm A}$ is a measure of the cross section

$$\frac{d\sigma}{d\epsilon_{\rm A}} = \sum_{n=n_{\rm min}}^{\infty}\frac{d\sigma_n}{d\epsilon_{\rm A}} + \int_0^\infty \frac{d^2\sigma}{d\epsilon\, d\epsilon_{\rm A}}\,d\epsilon, \qquad (3)$$

which must be convoluted with the spectrometer window function for comparison with the experimental data. If the final double-hole–state lifetime Γ_f^{-1} is taken into account, the Dirac delta function in Eq. (1) is replaced by the normalized density function

$$(\Gamma_f/2\pi)[(\omega-\epsilon-\epsilon_{\rm A}-I_{ff'})^2+\Gamma_f^2/4]^{-1}.$$

It follows from Eqs. (1) and (2) that for $E_{\rm exc} > 0$ the discrete part of the cross section (3) rapidly vanishes compared with the continuum part $d\sigma_c/d\epsilon_{\rm A}$. In the limit $\Gamma_i \rightarrow 0$, the corresponding overlap integral $\langle\epsilon|\tau'\rangle$ can be approximated by taking the overlap between two WKB wave functions, corresponding to $\frac{1}{2}k_i^2 = E_{\rm exc} + i(\Gamma_i/2) + V_i(R)$ and $\frac{1}{2}k_f^2 = E_{\rm exc} - \epsilon_{\rm A} + \epsilon_{\rm A}^0 + V_f(R)$, respectively.[2] We have $V_f = 2V_i = R^{-1}$, where the angular-momentum exchange between the photoelectron and the Auger electron is neglected. All semiclassical models of PCI seem to be variants of the WKB approximation, limited to the very-high-n and continuous-ϵ region. Qualitatively, both Eqs. (1)–(3) and the semiclassical approach lead to a transfer of intensity from the low-energy to the high-energy flank of the Auger-electron peak, compared with a Lorentzian shape, resulting in a positive PCI shift Δ. However, whereas in the semiclassical approach the regime $\epsilon_{\rm A} - \epsilon_{\rm A}^0 \gtrsim E_{\rm exc}$ ($\epsilon < 0$) is approached by analytic continuation, the quantum-mechanical theory leads to a spectator-line structure, important in practice for $E_{exc} \lesssim 2\Gamma_i$.

The derivation of Eq. (1) from the general transition-matrix formula[4] is based on a number of approximations. The most severe of these is probably the factorization of the many-electron Hamiltonian matrix element that involves the final two-electron scattering wave function into the one-electron overlap element $\langle\epsilon|\tau\rangle$ and the Auger-electron probability amplitude.

The cross section (3) was calculated for the L_3-M_4M_5 ($^1G_4$) transition with the use of Hartree-Fock (HF) wave functions. Calculation of the continuous part of the function (2) required, for each E_{exc} (3, 10, and 20 eV), 2 000 continuum wave functions $|\tau d\rangle$ in steps of 0.1 eV. These wave functions, as well as the final-state continuum wave functions $|\epsilon d\rangle$, were generated in the configuration-average frozen HF core, with the exchange interaction taken into account. The summation over the discrete intermediate states was found to be negligible in all three cases.

The ~ 2.3-eV width of the spectrometer window allows us to resolve only the $5d$ spectator line in the range -8 eV $< E_{exc} < +5$ eV, at $\Delta(5d) = E_{exc} + 10.5$ eV, from the rest of the structure which appears as a single peak at $\Delta < \Delta(5d)$. Up to $E_{exc} = 0$ eV, Δ appears to follow a linear dispersion law, $\Delta = E_{exc} + 4.0$ eV, which indicates that it is mostly $6d$. The linear dependence of $\Delta(5d)$ and $\Delta(6d)$ on E_{exc} is plotted in Fig. 2; the resonance energies are indicated at which the spectator lines gain maximum intensity. According to Eqs. (1)–(3), these resonances occur at $E_{exc} = -\tau_n$ or $\Delta(nd) = \epsilon_n - \tau_n$. The measured energies τ_n agree well with relaxed HF calculations for $n = 5$ and 6.

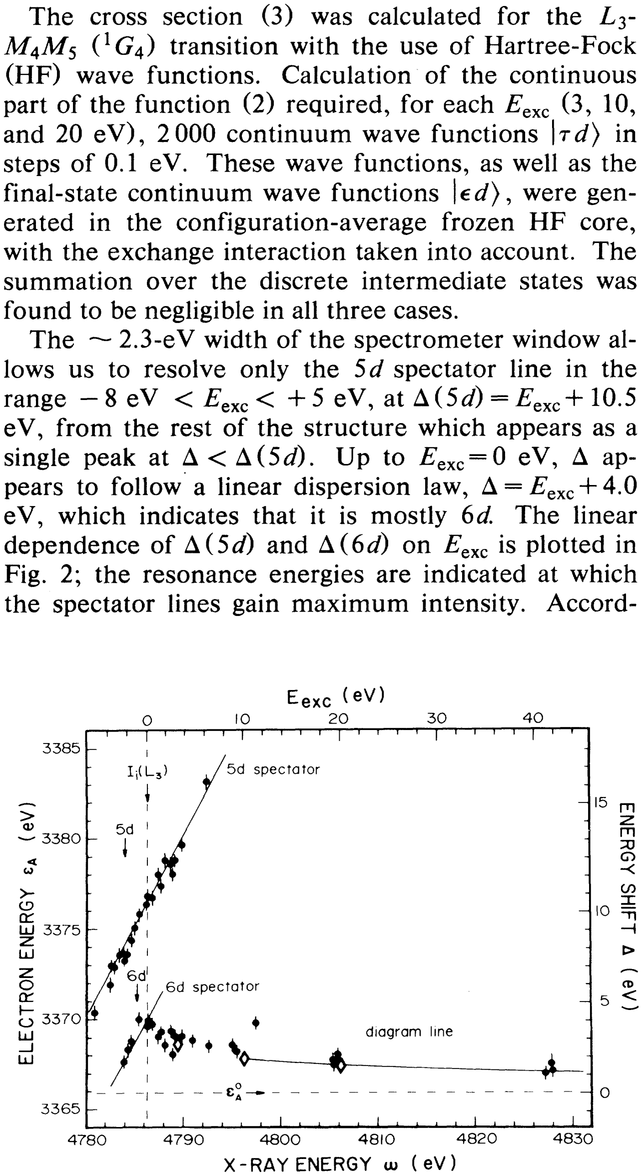

FIG. 2. Xenon L_3-M_4M_5($^1G_4$) Auger-electron-peak energies, as functions of excitation energy. Experimental data are indicated by solid circles. Lozenges represent the quantum-mechanical shift Δ of the diagram line, while the solid curve indicates the semiclassical shift.

The measured width of the $5d$ and $6d$ spectator lines is 4.0 ± 0.5 eV, independently of E_{exc}. This is clearly narrower than the natural width of the L_3-M_4M_5 ($^1G_4$) line ($\Gamma_i + \Gamma_f \cong 4.2$ eV),[7] convoluted with the 2.3-eV-wide spectrometer window, i.e., 5.3 eV. This resonance narrowing is in accordance with Eqs. (1)–(3) which, in analogy with the x-ray resonant Raman case,[5] predict $d\sigma_n/d\epsilon_A \propto N(\omega - \omega_0)$, where $N(\omega - \omega_0)$ is 0.6 eV wide in our experiment.

With the sum rule $\int |\langle\epsilon|\tau'\rangle|^2 d\epsilon = \langle\tau'|\tau'\rangle$, where summation over discrete states is included, it is possible to estimate how much of the low-energy structure represented by peak C in Fig. 1 is due to spectator states. The result, in agreement with the gradual, slow disappearance of the $5d$ spectator line, is that for $E_{exc} \lesssim 2\Gamma_i$, the contribution from the discrete final states cannot be neglected. Hence $E_{exc} = +3$ eV represents an intermediate case, in which there is an apparent shift due to the spectators. Experimentally we find $\Delta = 3.0 \pm 0.5$ eV, whereas theory predicts $\Delta = 2.8$ eV after convolution with the final-state density and the spectrometer window function.

In the calculation of $d\sigma_n/d\epsilon_A$, the discrete portion of complete-set HF computations was approximated by quantum-defect theory for both n' (intermediate) and n (final) states $\geqslant 8$. The summation over intermediate continuum states was found to be important, indicating that there is appreciable recapture of the photoelectron into Rydberg states.

For $E_{exc} \gtrsim 5$ eV, the quantum-mechanical shape of the Auger diagram line agrees closely with that obtained from the semiclassical Niehaus theory[2] through numerical integration. After convoluting the theoretical shapes, we find the shifts $\Delta_{theory} = 2.0$ eV, $\Delta_{expt} = 2.5 \pm 0.5$ eV for $E_{exc} = 10$ eV, and $\Delta_{theory} = 1.6$ eV, $\Delta_{expt} = 1.9 \pm 0.7$ eV for $E_{exc} = 20$ eV. It remains to be shown analytically why the Niehaus theory,[2] if the stationary-phase approximation is not invoked,[8] leads to almost identically the same results as the quantum-mechanical approach. In Fig. 2, the solid curve for the diagram-line energy represents the function $\Delta = \Delta(E_{exc})$, obtained from the Niehaus theory and convoluted.

Similar measurements as here described have been performed on other wide inner-shell hole states.[9] Computations are in progress to apply the resonant scattering theory[4,5] to these cases as well.

We gratefully acknowledge technical support at Stanford Synchrotron Radiation Laboratory from Hans Przybylski, Teresa Troxel, and Glen Kerr. We are indebted to William F. Ballhaus, Jr., and David M. Cooper for facilitating the performance of major computations in the NASA Ames Research Center, and to Mei Chi Chen for assistance with these computations. We thank Kh Rezaul Karim for helpful conversations. This work was supported in part by the Advanced Research Projects Agency of the Department of Defense, monitored by the Air Force Office of Scientific Research under Contract No. F49620-84-C-0039 with the University of Oregon, and by the U. S. Department of Energy. The Stanford Synchrotron Radiation Laboratory is supported by the Department of Energy through the Office of Basic Energy Sciences and by the National Institutes of Health through the Biotechnology Resources Program.

[(a)]Permanent address: Laboratory of Physics, Helsinki University of Technology, 02150 Espoo 15, Finland.

[1]G. S. Brown, M. H. Chen, B. Crasemann, and G. E. Ice, Phys. Rev. Lett. **45**, 1937 (1980).

[2]A. Niehaus and C. J. Zwakhals, J. Phys. B **16**, L135 (1983), and references therein.

[3]M. Ya. Amusia, M. Yu. Kuchiev, and S. A. Sheinerman, in *Coherence and Correlation in Atomic Collisions,* edited by H. Kleinpoppen and J. F. Williams (Plenum, New York, 1980), p. 297.

[4]T. Åberg, in *Inner-Shell and X-Ray Physics of Atoms and Solids,* edited by D. J. Fabian, H. Kleinpoppen, and L. M. Watson (Plenum, New York, 1981), p. 251.

[5]T. Åberg and J. Tulkki, in "Atomic Inner-Shell Physics," edited by B. Crasemann (Plenum, New York, to be published), Chap. 10.

[6]We follow the convention of denoting hole states by square brackets, and use atomic units throughout.

[7]The width $\Gamma_i = 2.82$ eV was taken from M. H. Chen, B. Crasemann, and H. Mark, Phys. Rev. A **24**, 177 (1981); $\Gamma_f \cong 1.4$ eV was estimated from the Xe $3d$ photoelectron linewidth as given by U. Gelius, J. Electon Spectrosc. Relat. Phenom. **5**, 985 (1974).

[8]This approximation has recently been discussed by A. Russek and W. Mehlhorn, to be published.

[9]G. E. Ice, G. S. Brown, G. B. Armen, M. H. Chen, B. Crasemann, J. Levin, and D. Mitchell, in *X-Ray and Atomic Inner-Shell Physics—1982,* edited by B. Crasemann, AIP Conference Proceedings No. 94 (American Institute of Physics, New York, 1982), p. 105.